



**HAL**  
open science

# Optically stimulated phosphorescence in quartz over the millisecond to second time scale: insights into the role of shallow traps in delaying luminescent recombination

C Ankjaergaard, M Jain

## ► To cite this version:

C Ankjaergaard, M Jain. Optically stimulated phosphorescence in quartz over the millisecond to second time scale: insights into the role of shallow traps in delaying luminescent recombination. *Journal of Physics D: Applied Physics*, 2010, 43 (25), pp.255502. 10.1088/0022-3727/43/25/255502 . hal-00569634

**HAL Id: hal-00569634**

**<https://hal.science/hal-00569634>**

Submitted on 25 Feb 2011

**HAL** is a multi-disciplinary open access archive for the deposit and dissemination of scientific research documents, whether they are published or not. The documents may come from teaching and research institutions in France or abroad, or from public or private research centers.

L'archive ouverte pluridisciplinaire **HAL**, est destinée au dépôt et à la diffusion de documents scientifiques de niveau recherche, publiés ou non, émanant des établissements d'enseignement et de recherche français ou étrangers, des laboratoires publics ou privés.

# Optically stimulated phosphorescence in quartz over the millisecond to second time scale: insights into the role of shallow traps in delaying luminescent recombination

C. Ankjærgaard\*, M. Jain

Radiation Research Division, Risø National Laboratory for Sustainable Energy, Technical University of Denmark, DK-4000 Roskilde, Denmark.

\*Corresponding author; email: christina.ankjaergaard@gmail.com; Telephone: +45 4677 4920

## ABSTRACT

Time-resolved OSL curves from quartz are usually measured over a few hundred  $\mu\text{s}$  because this time range best illustrates the main component in quartz which lies in the range of 30-45  $\mu\text{s}$ . In this study we present the decay form of quartz time-resolved optically stimulated luminescence (TR-OSL) and optically stimulated phosphorescence (OSP) covering over 8 orders of magnitude from 50 ns to  $\sim 8$  s. A detailed characterisation of the previously unstudied slowly decaying signals (ms-s time scales) is undertaken to understand the origin of these components and the role of re-trapping following optical stimulation. We present preheat and stimulation temperature dependence for both the TR-OSL and OSP curves in these time ranges and use the latter data to determine the E and s values for the participating shallow traps. We observe an abnormal decay behaviour seen as a sudden increase in the decay rate (a 'kink') conspicuous at about 2 – 3 s in the OSP curves measured at 75 and 100°C. We satisfactorily reproduce this behaviour with a numerically solved kinetic model consisting of 4 energy levels. The physical interpretation of the kinetic rate equations is discussed in terms a three trap – one centre model or a one trap – two centres model involving localised charge transfer.

## KEYWORDS

Quartz, Optically Stimulated Luminescence (OSL), Time-Resolved OSL (TR-OSL), Optically Stimulated Phosphorescence (OSP), Delayed OSL (DOSL), Photo-Transferred Thermoluminescence (PTTL), 110°C TL trap, kinetic model

## 1. INTRODUCTION

Natural quartz is widely used in luminescence based retrospective dosimetry (Bøtter-Jensen et al., 2003a). The luminescence from previously beta or gamma irradiated quartz can be obtained by thermal, or by continuous or pulsed optical stimulation. In pulsed optical stimulation mode the luminescence measured during and between the pulses is known as Time-Resolved OSL (TR-OSL) and can be used to understand the various recombination routes in a crystal. TR-OSL of quartz has been studied for almost a decade (Bailiff, 2000; Chithambo and Galloway, 2000; Chithambo et al., 2007; Pagonis et al., 2009, and references in these papers).

The main processes that govern the time scales involved in optically stimulated luminescence generation are generally exponential in nature. The most important of these processes are: (a) detrapping: eviction of a trapped electron by stimulation to the conduction band, (b) transition from the conduction band to the luminescence centre, and (c) the relaxation from the excited state to the ground state of the luminescence centre.

The rates of each of these processes are in turn determined by the lifetimes of the electrons in transition from one energy level to the other. During optical detrapping the mean life of a trapped electron is determined by the photoionisation cross-section of the trap. In pulsed stimulation where the luminescence signal is analysed after the pulse, i.e. in the off-time, process (a) can be eliminated and moreover it can be assumed that there is negligible change in the concentration of recombination centres as the energy delivered to the sample during a pulse is rather small. Thus, the relevant parameter related to process (b) is the mean life of the electrons in the conduction band. This lifetime would normally determine the lifetime of the luminescence decay. However, in cases, where, depending on the nature of the centre, the recombination leads to an excited state there is another delay in the luminescence production; a photon is only released after relaxation from the excited to the ground state of the centre, process (c). The excited state lifetime is a characteristic of the recombination

centre and is determined by the excited state to ground state transition, e.g., whether it is forbidden (resulting in a long lifetime) or allowed (resulting in a short lifetime). Thus, in pulsed OSL measurements the decay form of luminescence measured in the off-time will be a combined effect of two exponential functions, namely (b) and (c) (we note that we do not discuss localised transitions or tunnelling effects here). The timescales involved can be from ns to up to several tens of ms. However, on longer timescales, re-trapping and thermal emptying of the shallow traps can become important and give rise to long lived phosphorescence.

Examination of the luminescence decay after a pulse of stimulation light helps to understand the relative role of the above processes in luminescence generation. Different terminologies have been used to name such a signal, e.g. Time-Resolved OSL (TR-OSL), Delayed OSL (DOSL) or optically stimulated phosphorescence (see Bøtter-Jensen et al. 2003a, p59-60). One could argue that the term TR-OSL is generally used when a train of pulses is used as an alternative to CW-OSL, whereas the terms DOSL or optically stimulated phosphorescence (OSP) or afterglow refer to measurements in which a single or a few short stimulations (ms to s) are followed by extended examination of the subsequent luminescence signal over ms to s time scales, such that the afterglow is resolvable by the human eye.

Quartz TR-OSL measured between the stimulation pulses (after preheating to 260°C for 10 s and stimulating at 125°C) shows a monotonic decay and consists of a dominant exponential transient having a lifetime between 30 and 45  $\mu$ s and two relatively minor transients having relatively shorter and longer lifetimes (Chithambo et al., 2007; Ankjærgaard et al., 2010). These lifetimes most likely reflect the relaxation of the excited state following electron hole-recombination (Chithambo, 2007; Pagonis et al., 2010). Almost all published TR-OSL off-time decay curves from quartz have been measured over a few hundred microseconds (Chithambo et al., 2008 and references therein; Ankjærgaard et al., 2010). However, on longer time scales it is likely that the effect of re-trapping will also be apparent. For example, Markey et al. (1995) using  $\text{Al}_2\text{O}_3:\text{C}$ , demonstrated that the main lifetime of  $\sim 35$  ms corresponds to the decay of the excited F-centre in  $\text{Al}_2\text{O}_3:\text{C}$ , but that the much slower decay of  $\sim 545$  ms (measured at 25°C) is due to phosphorescence from transfer of charge from deep traps to shallow traps. As these shallow traps are thermally unstable at room

temperature, they start to leak charge into the conduction band from where it recombines and emits light (DOSL - Bøtter-Jensen et al., 2003a).

Only few measurements have been done to study the TR-OSL decay from quartz on the ms to s timescales. Pagonis et al. (2009) show an example from high purity synthetic quartz obtained for an off-time of 1 ms. The authors identify a slow component within this sample with a lifetime of  $14 \pm 8$  ms and surmise that it could be caused by re-trapping in a shallow trap. This effect has previously been used by Jaek et al., (1999) to investigate deep traps in quartz, although here it was called Optically Stimulated Afterglow (OSA).

In this study we first establish the decay form of optically stimulated phosphorescence in irradiated quartz using different techniques to cover time scales over >8 orders of magnitude (50 ns to ~8 s). We then make a detailed characterisation of the hitherto unstudied slowly decaying signals (ms-s time scales) to understand the origin of these components and the role of re-trapping following the optical stimulation.

We use the terminology time-resolved OSL (TR-OSL) while referring to the ns -  $\mu$ s time scales and optically stimulated phosphorescence (OSP) while referring to the ms - s time scales.

## **2. EXPERIMENTAL DETAILS**

Sample measurements were carried out on two different Risø readers to cover three different time scales. Optical stimulation carried out using blue light and detection was through a 7.5 mm thick Hoya U340 filter used for detection. The measurement details are described below.

**Nanoseconds – microseconds:** A Risø TL/OSL-20 reader was used with an integrated pulsing option to control the blue LED array, delivering  $80 \text{ mW.cm}^{-2}$  CW stimulation at the sample position. Furthermore a Photon Timer was attached, based on an ORTEC 9353 100 ps Time Digitizer board with a detection resolution (bin-width) of 100 ps to record the TR-OSL (Lapp et al., 2009). We define the duration of each stimulation LED pulse as the on-time, and the duration of the pause before the next stimulation pulse as the off-time (see also Lapp et al., 2009). Measurements on

this timescale were undertaken using an on-time of 50  $\mu\text{s}$  and an off-time of 500  $\mu\text{s}$  producing  $\sim 40,000$  stimulation pulses during 22 s of pulsed stimulation with an energy of  $3.6 \mu\text{J}\cdot\text{cm}^{-2}$  per pulse.

**Microseconds – milliseconds:** The same Risø TL/OSL-20 reader as above was used but with an on-time of 1 ms and an off-time of 5 ms. The ORTEC board has a pulse period (on-time + off-time) limitation of 6 ms, which currently cannot be exceeded. Approximately 9,000 pulses with an energy of  $72 \mu\text{J}\cdot\text{cm}^{-2}$  per pulse were delivered during 54 s of pulsed stimulation in this time range.

**Milliseconds – seconds:** A standard Risø TL/OSL-15 reader with CW stimulation system performed by a LED array delivering  $\sim 40 \text{ mW}\cdot\text{cm}^{-2}$  CW stimulation at the sample position (Bøtter-Jensen et al., 2003b) was used to produce a single light pulse of 0.2 s duration with an average energy of  $6.7 \text{ mJ}\cdot\text{cm}^{-2}$ . The phosphorescence was detected during the following 7.8 s.

The on- and off-times mentioned above were adhered to unless otherwise specified in the text.

The work reported here has been undertaken using 90-125  $\mu\text{m}$  sedimentary quartz grains (lab code: WIDG8). The quartz grains were extracted from the sample by sieving, heavy liquid separation and HF treatment as described in Wintle and Murray (1997) and the absence of significant feldspar contamination was confirmed by tests using IR stimulation. All aliquots used consisted of grains mounted in steel cups using silicon oil.

### **3. EXTENDED DECAY FORM OF OPTICALLY STIMULATED PHOSPHORESCENCE FROM QUARTZ**

Time-resolved OSL off-time curves from quartz are usually measured over a few hundred  $\mu\text{s}$  because this time range best illustrates the main component in quartz which has a lifetime in the range of 30-45  $\mu\text{s}$ . In Fig. 1(a), this is illustrated by the black curve, which has been measured at  $125^\circ\text{C}$  after a 25 Gy dose and a preheat to  $260^\circ\text{C}$  for 10 s. The same curve is shown in Fig. 1(b) on a semi-log scale, where this

main component can be seen as the linear part of the curve up to  $\sim 150 \mu\text{s}$ , after which a much slower decaying component starts to dominate.

To observe in detail the slowly decaying part of the decay, the measurement was repeated on the millisecond timescale, which is shown as the red curve in Fig. 1(a) and reproduced in Fig. 1(c) on a semi-log scale; the initial fast drop corresponds to the main component from Fig. 1(b) marked by #1, followed by the same slowly decaying component from 1(b) marked by #2, but now it is clear that the decay continues beyond several ms, as the counts have still not reached the background level of  $\sim 4$  cts. per channel ( $6.6 \mu\text{s}$ ).

To make further extended measurements of the slowly decaying component, a measurement was carried out in the standard Risø reader with the CW-OSL attachment using a single pulse of blue stimulation. The measurement and preheat temperatures were the same as above. These data are shown as the last (blue) curve in Fig. 1(a) and on a semi-log scale in Fig. 1(d). The initial fast drop is termed as component #3, and continues up to about 2 seconds, after which it is hidden under a new component marked as #4 which continues beyond 7 s. The dark counts in this curve will occur at  $\sim 0.2$  cts. per channel ( $0.002$  s)

We note that the components 1, 2, 3 and 4 mentioned above are defined entirely based on visual inspection. Due to lack of data collected from 6 ms up to  $\sim 60$  ms, we cannot know whether component 2 and 3 are the same or not. The mosaic of these curves in Fig. 1(a) illustrates that the TR-OSL or OSP covers  $>8$  orders of magnitude ( $50$  ns to  $\sim 8$  s). The lower limit of this observation is set by the incapability of our set up to achieve pulsing with a diode fall time faster than  $\sim 20$  ns. The upper limit is set by the instrument's sensitivity; we are already quite close to the dark counts of the system by about 8 s of OSP measurement.

In the following sections we make a detailed characterisation of these components with a special focus on 2, 3, and 4.

#### **4. THE MICROSECOND - MILLISECOND (ms) TIME RANGE**

This section investigates the shape of the curve in Fig. 1(c) as a function of preheat and stimulation temperature. Fig. 2 shows the normalized time-resolved OSL off-time curves measured at 125°C from a single aliquot of quartz using preheat temperatures in the range 200-300°C. It is observed that the preheat temperature does not affect the shape of the curve. The amplitude of the initial component 1 (filled circles) and the slower component 2 (estimated from the intensity at 1 ms, open circles) are shown in the figure inset as a function of preheat temperature. There is no major change in the relative importance of the two components with preheat temperature.

The normalized blue light stimulated time-resolved OSL from a single aliquot of quartz (WIDG8) measured for stimulation temperatures in the range 50-225°C are shown in Figure 3(a). Only the off-time decay is shown. As the stimulation temperature is increased, the area under component 2 shows an increase relative to that under component 1. For the curves with stimulation temperatures below 125°C, the initial decay has a very similar behaviour (see inset to Fig. 3(a) on log-log plot) and the relative ratios between the two components are very similar. For the curves with stimulation temperatures above 125°C, the initial decay becomes faster with increasing temperature, and the slower decay becomes relatively more dominant.

We tried to describe these data mathematically by a multi-exponential fit. However, the curves were not successfully described by either two or three or more transients, possibly because of very large difference in decay constants (microsecond and millisecond) causing an abrupt change in the decay curves (Fig. 3a). Therefore in order to study the main characteristics of the curve, we used the very initial part of the curve to characterise component 1. Fig. 3(b) shows the lifetime and amplitude for this component. For characterisation of component 2 we discarded the initial 400  $\mu$ s of data in the off-time (to remove nearly all influence of the initial fast decay) and thereafter removed the contribution from the underlying slower components (component 3 and 4, see Fig. 1) by subtraction of an average over the last 50 points. The remaining data were satisfactorily approximated with a single exponential decay. The lifetime and amplitude of this component as a function of temperature is shown in Fig. 3(c).

Component 1, the dominant component at the microseconds (and also the milliseconds) time scales in quartz (Ankjærgaard et al., 2010), shows a decrease in both the amplitude and lifetime as a function of temperature (Fig. 3b). The decrease in amplitude and lifetime with stimulation temperature can be ascribed to thermal quenching (Fig. 3(b), triangles) which arises because of an alternative non-radiative recombination and has been studied in quartz by Bailiff (2000), Chithambo and Galloway (2001), and Chithambo (2002).

In (Pagonis et al., 2010), thermal quenching was measured and modelled for the same quartz sample as used here (WIDG8). A decrease in lifetime of  $\sim 45 \mu\text{s}$  to  $\sim 10 \mu\text{s}$  observed here (Fig. 3b) for the temperature range  $50^\circ\text{C}$  to  $200^\circ\text{C}$  is consistent with the thermal quenching energy of 0.64 eV (See Pagonis et al. 2010 for the details).

Component 2 shows a relatively smaller decrease in intensity than component 1 with an increase in the stimulation temperature; the smaller decrease in the amplitude compared to that of component 1 causes the observed changes in the relative contributions from the two components in Fig. 3(a). However, unlike component 1, the lifetime does not decrease concomitantly with the amplitude. In fact the lifetimes show only a slight change for the different stimulation temperatures up to  $200^\circ\text{C}$ ; there is an overall 38% increase in lifetime with temperature up to  $200^\circ\text{C}$ , with a single reproducible dip at  $100^\circ\text{C}$ , followed by a sharp drop of about 50% between  $200^\circ\text{C}$  and  $225^\circ\text{C}$ . Thus the lifetime of component 2 does not show an undisputed constancy, or a systematic decrease expected from faster emptying of shallow traps or greater thermal quenching at a centre such as observed for component 1. One possible explanation could be that the so called component 2 in fact has different origins at different temperatures and therefore, it is not valid to intercompare the lifetimes; the apparent similarity in the lifetimes is then a mere coincidence. We later describe such an apparent behaviour in a component in the time range described in Section 5. On the other hand if one ignores the drop at  $100^\circ\text{C}$ , one could possibly assume a near constancy of the lifetimes between 50 to  $200^\circ\text{C}$  as a gross simplification. We discuss this again in the later sections.

## **5. THE MILLISECOND - SECOND TIME RANGE**

Because of the ORTEC board pulse period limitation of 6 ms, the components in this range were investigated using a conventional reader by giving a single stimulation pulse of 0.2 s and measuring the following phosphorescence decay for 7.8 s.

### 5.1 Preheat and Stimulation temperature dependence

To investigate the off-time signal behaviour as a function of preheat, a series of curves were measured at 125°C using an aliquot of quartz following a single stimulation pulse, these are shown in Fig. 4, all normalized to the initial point in the off-time. All curves behave identically with a fast drop in the initial 0.01 s (see also inset on log-log scale), a slower decay up to about 1 s where the slowest decay starts to dominate and continues beyond 7 s. Based both on this and the  $\mu$ s to ms data presented in the previous section, we conclude that the preheat temperature range (200 to 300 °C) does not affect the relative contributions of the different components. Fig. 5(a) shows the stimulation temperature dependent decay of the same aliquot of quartz used in Fig. 4. The aliquot was heated to 260°C for 10 s prior to blue light stimulation at temperatures in the range 50 – 200°C. The curves show very different decay rates during the initial 3 s (see a magnification of this time range in Fig. 5(b)). However, in the data following the 3 s (Fig. 5(a)) the decay shapes are very similar for all the temperatures, with an exception of the 100°C curve (green triangles) and to some extent the 75°C curve (red squares) where a clear ‘kink’ is observed at ~3 s.

A clearer picture can be obtained by separating the different components. Because of the ‘kink’ in two of the curves (75 and 100°C), we could not apply a simple multi-exponential model to the entire curve. Therefore, to simplify the analysis we fitted only the data in the first 3 s assuming first order kinetics (see Fig. 5b). The data were successfully fitted with a sum of three exponentials. To determine the effect of temperature, an Arrhenius plot is used, which is shown in Fig. 6(a). The three different components from each curve are indicated by different symbols (Fast – circles, medium – triangles, slow – squares). If one looks at the behaviour of these different components, it is apparent that the lifetime of the slow and medium component do not vary much with temperature, whereas the lifetime of the fastest component rises gradually with temperature up to 150°C ( $\sim 28 \text{ eV}^{-1}$ ), and then decreases rapidly between 150 – 200°C ( $28 - 24 \text{ eV}^{-1}$ ). The behaviour of these components is in fact very similar to that observed for component 2 on the ms time

scales (see previous section, Fig. 3(c)) in that it does not show any obvious temperature dependence.

We now explore the possibility that the fast component (and similarly the medium component and slow component) actually has different origins in these different curves. If one looks closely at Fig. 5(b), i.e. the data in the first three seconds of the curves in Fig. 5(a), then it is apparent that a slower component increases relatively in magnitude compared to a faster decaying component from about 50 to 100°C, and the fast component is eliminated above 100°C. From 100°C to 175 °C one also observes a systematic change in the decay rate of the dominant component with stimulation, which hints to a possible participation of a shallow trap(s). A common dominant component of these different curves was picked by visual inspection. This is shown by arrows and lettering from a-f for the different curves in Fig. 5(b). It is clear that this component shows an increase in the decay rate with temperature; however, note that in some curves this is a slow component while in the others it is a fast component. The Arrhenius plot helps to test whether the change in the decay rate complies with that expected from thermodynamic considerations. Most of the data for this component does in fact fall on a straight line (red line in Fig. 6(a))  $\tau = E/kT - \ln(s)$ , where  $\tau$  [s] is the lifetime,  $E$  [eV] is the thermal activation energy of the trap giving rise to this component, and  $s$  [ $s^{-1}$ ] is the frequency factor. This gives  $E = 0.91$  eV and  $s = 1.7 \cdot 10^{12} s^{-1}$ . Very similar values of  $E = 0.89$  eV and  $s = 3.8 \cdot 10^{11} s^{-1}$  were found by Spooner and Questiaux (2000) for the so called 110°C TL peak in the UV emission by varying the heating rate in a series of TL measurements. The  $E$  and  $s$  values found from our data predict a TL peak at 93°C for a heating rate of  $2^\circ C s^{-1}$  (confirmed later by experimental measurements).

Thus, identification of this main component helps to put the other two components derived from multi-exponential fitting into perspective. Examination of Fig. 5(b) again for temperatures below 100°C now shows that the component derived from the 110°C peak (marked with arrows) increases relative to the faster components and almost completely replaces these between 100°C and 125°C. Thus, these faster components are completely eliminated at higher temperatures, since the data resolution is not high enough to sample them. Similarly, as the component from the

110°C peak forms the new fast component, there is appearance of new slower components in the system. Thus, we conclude that the apparent constancy of the fast and medium components is misleading since the slower components change into faster ones, the faster ones disappear (or are unresolvable at our data collection rate), and the new slower components appear at higher and higher temperatures within our data range. It is therefore misleading to intercompare the decay rates for a single component as the decay rates should in fact be compared across components to obtain a meaningful result.

To confirm the role of the 110°C peak in OSP, a TL experiment was carried out to examine possible charge recuperation during short blue light stimulations; this is called phototransferred TL (PTTL). A previously sensitised aliquot was dosed, heated to 300°C for 60 s and then stimulated with a short pulse of blue light. Fig. 7 shows the series of 'difference' TL curves (subtraction of TL before illumination from that after illumination) measured up to 300°C following these short blue light stimulations of durations between 0.1 s and 3.2 s. The ~325 °C TL peak shows an increasing depletion because of bleaching by blue light; this is observed as negative counts in the figure. All positive counts are PTTL due to photo transfer. A dominant peak is observed at 97°C followed by relatively smaller peaks in the region between 125°C and 225°C. Increasing the stimulation pulse length causes an increase of charge transfer into the peak centred at 97°C, which is in reasonable agreement with our predicted TL peak at 93°C from the E and s values found from Fig. 6(a). The charge builds up steadily, but for pulse durations longer than 1.6 s, the light stimulation starts to deplete the charge transferred into this trap. Based on these data we conclude that our multi-exponential analysis as well our approach of comparing decay constants across the fast, medium, and slow components gives physically meaningful results.

With this success we then attempted a similar E-s analysis for the components decaying faster than that from the 110°C peak for the stimulation temperatures between 50 and 100°C. These are indicated with the blue, green, and grey dashed lines in Fig. 6(a). These yield values of E = 0.74 eV and  $s = 1.5 \cdot 10^{12} \text{ s}^{-1}$  (blue line), E = 0.86 eV and  $s = 2.9 \cdot 10^{13} \text{ s}^{-1}$  (green line), and E = 0.56 eV and  $s = 3.6 \cdot 10^9 \text{ s}^{-1}$  (grey line), which correspond to TL peaks at 87°C, 63°C, and 165°C respectively. In the

literature, only values for the 160°C peak are published with  $E = 1.09$  eV and  $s = 2.1 \cdot 10^{12} \text{ s}^{-1}$  measured in the UV (Spooner and Questiaux, 2000) We recognise that our  $E$  and  $s$  values for this peak are much too small compared to their published value, and moreover the  $s$  value is smaller than the generally accepted values in the range  $10^{12}$ - $10^{14} \text{ s}^{-1}$ . Nonetheless, our PTTL results in Fig. 7 show the existence of the 160°C TL peak, consistent with our E-s analysis.

The slower components (slower than that for the ~110°C peak) on the other hand do not seem to be amenable to this simple E-s analysis (See the data enclosed in the ellipse in Fig. 6(a)). Fitting of these data gave absurd values of  $E$  and  $s$ . Also a closer inspection of Fig. 5(b) suggests that at the higher temperatures the curve shape encompassing the medium and slowly decaying parts does not change significantly. We, therefore, infer that at about 150°C there appears a new component in our data that decays slower than the component induced from the 110°C peak, and that this new component does not show a significant change in the decay rate with stimulation temperature.

The latter part of the off-time decays from 3 to 7 s in Fig. 5(a) shows a similar decay rate for the different temperatures, except the curve measured at 100°C. A summary of the lifetimes are given in Fig. 6(b). The overall similarity in the decay rate for the different temperatures might suggest that this signal has a similar origin or is quite simply a continuation of the medium and slow components above (data shown in the ellipse, Fig. 6a).

The presence of the ‘kink’ at around 3 s (Fig. 5a) in the 100 and 75°C data is surprising. To our knowledge such a feature has not been reported before and suggests a rather different mechanism of luminescence generation, one that could possibly involve competition in the refuge (trap receiving charge from optical transfer) traps. This is examined in detail in the next sections.

## **5.2 ‘Kink’ position for different stimulation pulse durations**

To investigate whether the kink position is related to the amount of charge de-trapped from the OSL trap, measurements were carried out for different on-times at 100°C stimulation temperature after irradiation (25 Gy) and preheat (260°C for 10 s). Fig. 8

shows five curves with stimulation pulse durations (on-times) between 0.1 s to 1.6 s, and it is observed that the ‘kink’ occurs sooner for the longer on-times. A summary of the ‘kink’ position is shown in the inset to the figure ranging from approximately 4 s for an on-time of 0.1 s to 1 s for an on-time of 1.6 s. We propose below a simple numerical model containing four energy levels to explain the possible origin of the kink structure in the OSP curve.

### 5.3 A three-trap one centre phosphorescence model

Fig. 9(a) shows a band model containing three traps  $T_1$ ,  $T_2$ ,  $T_3$  and a luminescence centre, L. The features of these traps are described below:

$T_3$ : An electron trap with negligible retrapping. Thus, the charge population decays exponentially at the ambient temperature. Non-retrapping is only an approximation to simplify the model and it is not critical to the model results. Majority of the charge released from  $T_3$  undergoes recombination at centre L, and a minor amount is trapped at  $T_2$ .

$T_2$ : This is a deeper electron trap (smaller decay constant at the ambient temperature than  $T_3$ ). It can either lose charge to the conduction band (and thereby cause electron-hole recombination at the centre L), or it can lose charge by localised transition to the trap  $T_1$ . The majority of the charge lost by  $T_2$  is taken by  $T_1$ ; this feature is the most critical aspect of the model which helps reproduce the observed kink in the data. For simplicity, since only a small fraction of the charge is released to the conduction band, we assume that it all undergoes recombination at the centre L and none of it is retrapped.

$T_1$ : This is the third trap in the system which receives the majority of charge released from  $T_2$  by localised transition. The charge released from  $T_1$  either undergoes a luminescent recombination with holes at L, or is re-trapped at  $T_2$  through the conduction band. Again it is not critical to the model whether  $T_1$  receives any electrons directly from the conduction band, not as far as it is only a minor amount compared to the charge received from  $T_2$ ; for convenience we have avoided this step.

The decay of electrons from these traps occurs due to the ambient temperature. The decay constants ( $\lambda$ ) are assumed to have the following relationship:  $\lambda_3 > \lambda_2 > \lambda_1$ ,

corresponding to T<sub>3</sub>, T<sub>2</sub> and T<sub>1</sub> respectively. At the end of the light stimulation these traps will have a certain initial concentration because of re-trapping from the conduction band, or as in the case of T<sub>1</sub> charge re-trapping from T<sub>2</sub>. Because of charge decay from T<sub>2</sub> with  $\lambda_2 > \lambda_1$ , charge will initially build up at T<sub>1</sub> prior to recombining at L. The rate equations describing this model for the off-time are given as:

$$\frac{dn_3}{dt} = -n_3\lambda_3 \quad \text{Equation 1}$$

$$\frac{dn_2}{dt} = -n_2\lambda_2 + f_3(n_3\lambda_3 + n_1\lambda_1) \quad \text{Equation 2}$$

$$\frac{dn_1}{dt} = -n_1\lambda_1 + f_2n_2\lambda_2 \quad \text{Equation 3}$$

$$I \propto (1 - f_3)(n_1\lambda_1 + n_3\lambda_3) + (1 - f_2)n_2\lambda_2 \quad \text{Equation 4}$$

Here  $I$  is the observed luminescence intensity at time  $t$ ,  $f_3$  denotes the fraction of charge from T<sub>3</sub> or T<sub>1</sub> re-trapped at T<sub>2</sub>, and  $f_2$  the fraction of charge from T<sub>2</sub> trapped at T<sub>1</sub>. Fig. 10 shows the phosphorescence contribution from T<sub>3</sub>, T<sub>2</sub>, and in T<sub>1</sub> together with the total phosphorescence when solving the above rate-equations with the parameters:  $n_{10} = 50 \text{ cm}^{-3}$ ,  $\lambda_1 = 0.04 \text{ s}^{-1}$ ,  $n_{20} = 300 \text{ cm}^{-3}$ ,  $\lambda_2 = 0.09 \text{ s}^{-1}$ ,  $n_{30} = 25 \text{ cm}^{-3}$ ,  $\lambda_3 = 0.3 \text{ s}^{-1}$ , and  $f_3 = 0.1$ , and  $f_2 = 0.92$ . The luminescence arising from the T<sub>3</sub> and T<sub>2</sub> traps (blue curve and green curve, respectively) shows an exponential decay with time, whereas that from the T<sub>1</sub> trap initially builds up to a maximum before it decays (see semi-log scale in Fig. 10(b)). The total emitted luminescence from L (black curve) being the sum of the light from T<sub>3</sub>, T<sub>2</sub>, and T<sub>1</sub> therefore decrease initially, but as the light originating from T<sub>1</sub> starts to dominate over the light originating from T<sub>3</sub> and T<sub>2</sub>, the total luminescence curve flattens out to a near constant level before the decay rate is increased again in accordance with the depletion of T<sub>1</sub>. This simulated behaviour with three traps appears very similar to the kink observed in the 100°C measurement in Fig. 5(a); it was furthermore observed in Fig. 5(a) that the kink disappears as the temperature is increased. From Fig. 5(b) and 6(a) we know that the lifetime of the 110°C TL trap decreases significantly (thereby an increase in the decay constant) for temperatures above 100°C. An increase in stimulation temperature would thus correspond to an increase in the decay constants  $\lambda_i$  in this model depending on the

exact E and s values for each level. For certain combinations of these values such that the increase in  $\lambda_1$  is greater than the increase in  $\lambda_2$  or  $\lambda_3$ , it is possible to remove the kink and instead have an apparent monotonic decay in the simulation results.

In Fig. 8 the kink was observed to shift position as a function of the stimulation pulse duration. This can be achieved in the model by changing the initial concentration of  $T_1$  ( $n_{10}$ ) at the end of the stimulation pulse. An increase in this initial concentration, as would be expected with an increase in the length of the stimulation pulse duration, causes the kink to move towards shorter times in the off-time. This behaviour is consistent with the data presented in Fig.8.

A simpler two trap model was also investigated using only  $T_2$  and  $T_1$  with  $\lambda_2 > \lambda_1$ . It is assumed that decay from both  $T_2$  and  $T_1$  produces light, and that a fraction of the charge from  $T_2$  is transferred into  $T_1$ . Similar to the model above, the two traps are filled during the light stimulation to have an initial charge concentration at the end of the stimulation of  $n_{20} > n_{10}$  after which they both start to decay. If  $f$  describes the fraction of charge transferred to  $T_1$ , then the rate equations describing this situation are given as:

$$\frac{dn_2}{dt} = -n_2\lambda_2 \quad \text{Equation 5}$$

$$\frac{dn_1}{dt} = fn_2\lambda_2 - n_1\lambda_1 \quad \text{Equation 6}$$

$$I \propto (1-f)n_2\lambda_2 + n_1\lambda_1 \quad \text{Equation 7}$$

Using the same values for  $n_{10}$ ,  $\lambda_1$ ,  $n_{20}$ , and  $\lambda_2$  as above, the series of curves in Fig. 11 shows the total phosphorescence emitted at L for different fractions,  $f$  between 0.1 and 1. The inset shows the behaviour of  $T_1$ ,  $T_2$  and L for  $f = 0.3$ , which is the green curve in the main figure. It is seen from these curves, that it is not possible to produce a kink with this simpler model; it is crucial that there are three distinct traps and that there is a step of almost complete charge transfer from one to the other.

#### 5.4 An alternative one-trap, two-centre phosphorescence model

The mathematical equations above (Eqn. 1-4) can equally be interpreted in terms of two different energy levels existing in a single centre. Here we propose an alternative interpretation of these equations. The model consists of a single trap,  $T_3$  with lifetime

$\lambda_3$ , and two luminescence centres  $L_a$  and  $L_b$ , where  $L_a$  has two excited states,  $L_{a1}$  and  $L_{a2}$ , (Fig. 9(b)). It is assumed that the relaxation from  $L_{a2}$  to  $L_{a1}$ , by  $\lambda_{a2}$  is non-radiative, but that the relaxation of  $L_{a1}$  to  $L_a$  (the ground state) by  $\lambda_{a1}$  is radiative. During a short light stimulation, charge is transferred to  $T_3$  and  $L_{a2}$ . In the off-time, a fraction of the charge from  $T_3$  recombines at  $L_b$  and the remaining recombines at the excited state  $L_{a2}$ . The equations describing this model are identical to Equations (1-4), with the slight modification that the charge loss from the  $L_{a1}$  state is entirely to the ground state (unlike in the electron trap model where there is partial loss from level  $T_1$  to level  $T_2$  as well), i.e. the value of  $f_2=1$ , the equations thus become:

$$\frac{dn_3}{dt} = -n_3\lambda_3 \quad \text{Equation 8}$$

$$\frac{dn_{a2}}{dt} = -n_{a2}\lambda_{a2} + f_3n_3\lambda_3 \quad \text{Equation 9}$$

$$\frac{dn_{a1}}{dt} = -n_{a1}\lambda_{a1} + n_{a2}\lambda_{a2} \quad \text{Equation 10}$$

$$I \propto n_{a1}\lambda_{a1} + (1 - f_3)n_3\lambda_3 \quad \text{Equation 11}$$

The results of these are almost identical to those in Fig. 10 because the retrapping terms in the trap model were very small (results not shown here). Again the key feature of this model is a non-luminescence relaxation from the level  $L_{a2}$  to  $L_{a1}$ , which produces the desired result.

The main difference between the two models is therefore not in the modelling results, but rather that they offer different advantages in the explanation of the data in Fig. 5(a) and Fig. 8. By choosing the one trap - two centres model, it is relatively easier to explain the temperature independence of the latter part (after 3 s) of the curves in Fig. 5(a), and perhaps also the component 2 in Fig. 3(c), as the relaxation from  $L_{a1}$  will dominate the curve after the kink, and this process can be temperature independent in the absence of thermal quenching. It would however require that the relaxation is strongly forbidden to cause delay on the seconds time scale; this needs to be investigated. The trap  $T_3$  could be similar to the 110°C TL trap, which dominates the early part of the phosphorescence curves, and this process is highly temperature

dependent. In this model the commonly observed 40  $\mu$ s component would be derived from the centre  $L_b$ .

## **6. PHOSPHORESCENCE CONTRIBUTION IN THE CW SIGNAL**

It is obvious that phosphorescence is negligible compared to the fast OSL component in quartz measured at 125°C. To evaluate how large the contribution of the phosphorescence decay is in a standard CW measurement of the slow component in quartz, a series of measurements were carried out where the phosphorescence was detected for 10 s following blue CW stimulations at 125°C for durations of 10 s to 70 s. From Fig. 7 it was evident that light stimulation caused photo-transfer of charge into the 110°C TL trap, but that for longer stimulations  $> 1.6$  s, the light started to erode the photo-transferred charge instead. To see if this is also true for very long stimulations, or if the phosphorescence signal builds up during long stimulations, the amount of phosphorescence during the 10 s off-time was summed and is presented in Fig. 12, where it has been normalized to the initial 10 s stimulation point. From this curve it is clear that the phosphorescence does not increase with increased stimulation time, initially there is a faster drop in signal, but at about 40 s, the amount of phosphorescence emitted reaches a near constant level independent of the stimulation time. The dashed line indicates the level of 'dark counts' in the PMT accumulated during 10 s after light stimulation (also normalized to the initial value as the other points) to show that the phosphorescence level is well above the dark count level. These data suggest that a fraction of the slow OSL component observed even at 125°C temperature may derive from decay of the refuge traps that initially store charge during OSL. In order to determine the % of the phosphorescence contained in the slow OSL signal, we calculated the ratio between the end point of the OSL signal and the first point in the phosphorescence signal (assuming that these points represent the equilibrium states at any time). This ratio is plotted for different stimulation times in the inset to Fig. 12. The fluctuations in the data reflect the low light levels. We note from these data that there may be a contribution from OSP of about 5 % in the slow OSL signal.

## **7. DISCUSSION**

We find that the shape of the TR-OSL or OSP curves is almost independent of the preheat temperature in the range of 200 to 300°C at all time scales investigated here.

This suggests that the refuge traps and centres participating in these processes must be the same irrespective of the preheat temperature. Moreover, the refuge traps must be emptied to the same relative levels for different preheats.

From our stimulation temperature data, a strong temperature dependence is seen in the initial 3 s of the phosphorescence curves in Fig. 5(b). An E-s analysis of this changing component using an Arrhenius plot finds the trap depth  $E = 0.91$  eV to be consistent with that found for the 110°C TL trap of  $E = 0.89$  eV by Spooner and Questiaux (2000), and using our E and s values, a TL peak is predicted at 93°C for a heating rate of  $2$  °Cs<sup>-1</sup>. This is further confirmed by TL measurements showing a PTTL peak at 97°C. The phosphorescence we observe during the initial 3 s of the curves is, therefore, dominated by charge recycled through the 110°C TL trap. This conclusion is consistent with the previous studies on PTTL in quartz (see Wintle and Murray 1997 and references therein). Wintle and Murray (1997) also show for their quartz (WIDG8) the photo-transferred TL (PTTL) at room temperature illumination. In the absence of saturation effects, the ratio of 110°C PTTL to OSL is between 4 and 5% (Wintle and Murray, 1997).

In addition to the OSP component derived from the 110°C peak, we also find that there are some components both at the millisecond and second time scales that do not show an obvious dependence of their decay rates on the stimulation temperature. One possible reason for this could simply be, that we have not recorded data for sufficiently long time (e.g. in the milliseconds time scale) to track the movement of the different components. Another possible explanation could be the lack of a good mathematical model to extract individual components from the data; it is likely, as shown in the numerical modelling results, that the data do not follow a multiple-exponential form of the type used here for fitting. Thus, the apparent non-dependence on temperature could possibly be an artifact of our assumption that the OSP consists of linear superimposition of first-order processes. However, we note that the decay of the 110°C peak is conspicuous and has been picked up accurately by the fitting analysis (as confirmed by E and s values from Spooner and Questiaux, 2000). Similarly, the occurrence of a 160°C TL peak from the fitting analysis is supported by the PTTL data. We, therefore, consider that our analysis of the first 3 seconds of the data may be relatively error free, especially for the low temperature data (<125°C, Fig.

6(a)); the more problematic region may be the medium and slow components observed above 125°C (and the OSP data >3 s) as these could fall in the region where a peak build-up is predicted from the kinetic model (discussed below).

Two simple kinetic models are proposed to explain an abnormal change in the decay rate (the 'kink') in the OSP signals for the 75° and 100 °C stimulation temperatures (Figs. 5a and 8). The first model consists of three traps and a luminescence centre, while the second model consists of a single trap and two luminescence centres. The common trap  $T_3$  in both these models could be similar to the 110°C TL trap. Both models share the same equations (with minor modifications) and can, therefore, both predict the behaviour observed in Fig. 5(a). The key feature of both the models that produces the desired effect is a large non-luminescent transfer and subsequent build-up from one energy level to the other. The resultant luminescence has a peak shape, and this produces a flattening followed by a steep decay in the luminescence curve. An interesting prediction of our alternative model (one trap -two recombination centres) is that there could be OSP components which do not show a change in the decay rate with the stimulation temperature, thus strengthening the possibility that the effect discussed in the previous paragraph concerning data in Figs. 3 and 5 may be real and not just an artifact of the measurement or analysis. However, this implies a relaxation time in the centre on the seconds time scale, which may or may not be realistic. The model results are encouraging, but they need to be investigated in greater detail to understand different OSP results from quartz.

Finally, we note that a similar kink was also observed in the IR stimulated phosphorescence signals from orthoclase feldspar (Ankjærgaard and Jain, 2010). There and in the following paper (Jain and Ankjærgaard, 2010) it is shown that the slowly decaying signals (both on the ms and s time scales) arise from the slow emptying of the band tails. As in the case of quartz, these signals show a change in the amplitude but a weak dependence of lifetime on stimulation temperature. Although band tails have not been explicitly reported in quartz, it is possible that natural quartz contains band tails because of deformational strain in the source rocks. These effects are well known in common quartz bearing rocks, e.g. quartzite and granite. If band tail states are indeed present in our quartz, they could potentially give an alternative

explanation to the kink structure and temperature independence of the decay rates on the ms and s ( $>3$  s) time scales in quartz OSP.

## 8. SUMMARY AND CONCLUSIONS

1. The decay form of Time-Resolved OSL (TR-OSL) and Optically Stimulated Phosphorescence (OSP) in quartz has been observed to cover time scales of over 8 decades from 50 ns to  $\sim 8$  s.
2. The decay form of TR-OSL and OSP curves are independent of preheat temperature, for all the examined time scales, in the range 200-300°C suggesting that the same centres and refuge traps are used for all these conditions.
3. Together the TR-OSL and OSP curves have been shown to contain at least four major components (1-4) by visual inspection. Component 1 has an average lifetime of  $\sim 40$   $\mu$ s at room temperature; it shows strong temperature dependent decrease as expected from an excited state lifetime of a centre affected by thermal quenching. Component 2 has an average lifetime of  $\sim 1$  ms and shows no real systematic behaviour with temperature in our data range. Component 3 is strongly stimulation temperature dependent and has been identified mainly to originate from the 110°C TL trap, and partly from some other TL peaks determined to lie at 87°C, 63°C, and 165°C. Component 4 with an average lifetime of  $\sim 5$  s show an apparent overall temperature independence (with the exception at 100°C).
4. An abnormal decay behaviour (a 'kink') is observed conspicuously in the OSP data at 75°C and 100°C. A simple kinetic model consisting of four energy levels is proposed to explain the kink observed in the OSP data at around 3 s. This model can successfully reproduce the kink, and can be physically interpreted in terms of a 3 traps and 1 luminescence centre model, or alternatively, a 1 trap and 2 luminescence centres model with one of the centres having two excited states. The key feature of these models that produce the kink effect is a large localised, non-luminescent transfer and subsequent build-up from one energy level to the other. Although the results are encouraging, there needs to be further theoretical investigations into charge transfer and re-trapping to fully understand the optically stimulated phosphorescence results from quartz. One potential explanation for the

temperature dependence of lifetimes (components 2 and 4) as well as the kink structure could be the possible presence of band tail states in natural (deformed) quartz.

5. The 110°C TL peak plays a significant role even for optical stimulation at 125°C, although, the lifetime is rather small (0.2 s). It is determined that the OSP contribution to the OSL signal in the 10 s-70 s measurement region (for blue light stimulation at  $\sim 40 \text{ mW.cm}^{-2}$ ) is  $< 5\%$ . Although, this is unimportant for dosimetry, it could perhaps have a slight affect on the analysis of slow components in the slow OSL signals for derivation of physical parameters. A cleaner signal would be obtained by stimulations above 150°C, although at the cost of reduced sensitivity because of thermal quenching.

## ACKNOWLEDGEMENTS

We thank the two anonymous referees for a thorough review of the manuscript.

## 9. REFERENCES

Ankjærgaard, C., Jain, M., 2010. Optically stimulated phosphorescence in orthoclase feldspar over the millisecond to second time scales. Submitted to Journal of Luminescence.

Ankjærgaard C, Jain M, Thomsen K J, Murray A S, 2010 Optimising the separation of quartz and feldspar optically stimulated luminescence using pulsed excitation *Radiation Measurements*. In print. DOI: [10.1016/j.radmeas.2010.03.004](https://doi.org/10.1016/j.radmeas.2010.03.004).

Bailiff I K 2000 Characteristics of time-resolved luminescence in quartz *Radiation Measurements* **32** 401-405

Bøtter-Jensen L, McKeever S W S, Wintle A G 2003a *Optically Stimulated Luminescence Dosimetry* (Amsterdam: Elsevier) ISBN: 0-444-50684-5

Bøtter-Jensen L, Andersen C E, Duller G A T, Murray A S 2003b Developments in radiation, stimulation and observation facilities in luminescence measurements *Radiation Measurements* **37** 535–541

Chithambo M L 2002 Time-resolved luminescence from annealed quartz *Radiation Protection Dosimetry* **100** 273-276

Chithambo M L, Galloway R B 2000 A pulsed light-emitting-diode system for stimulation of luminescence *Meas. Sci. Technol.* **11** 418-424

Chithambo M L, Galloway R B 2001 On the slow component of luminescence stimulated from quartz by pulse blue light emitting diodes *Nuclear Instruments and Methods B* **183** 358-368

Chithambo M L 2007 The analysis of time-resolved optically stimulated luminescence: II. Computer simulations and experimental results *Journal of Physics D: Applied Physics* **40** 1880-1889

Chithambo M L, Preusser F, Ramseyer K, Ogundare F O 2007 Time-resolved luminescence of low sensitivity quartz from crystalline rocks *Radiation Measurements* **42** 205-212

Chithambo M L, Ogundare F O, Feathers J, Hong D G 2008 On the dose-dependence of luminescence lifetimes in natural quartz. *Radiation Effects and Defects in Solids* **163** 945-953

Jaek I, Hütt G, Streltsov A 1999 Study of deep traps in alkali feldspar and quartz by the optically stimulated afterglow *Radiation Protection Dosimetry* **84** 467-470

Jain M, Ankjærgaard C 2010 Towards finding a non-fading signal in feldspar: insight into charge transport and tunnelling from time-resolved optically stimulated luminescence *Radiation Measurements* submitted

Lapp T, Jain M, Ankjærgaard C., Pirzel L 2009 Development of pulsed stimulation and photon timer attachments to the Risø TL/OSL reader *Radiation Measurements* **44** 571-575

Markey B G, Colyott L E, McKeever S W S 1995 Time-resolved optically stimulated luminescence from  $\alpha$ -Al<sub>2</sub>O<sub>3</sub>:C *Radiation Measurements* **24** 457-463

Pagonis V, Mian S M, Chithambo M L, Christensen E, Barnold C 2009 Experimental and modelling study of pulsed optically stimulated luminescence in quartz, marble and beta irradiated salt *J. Phys. D: Appl. Phys* **42** 1-12

Pagonis V, Ankjærgaard C, Murray A S, Jain M, Chen R, Lawless J, Greilich S 2010 Modelling the thermal quenching mechanism in quartz based on time-resolved optically stimulated luminescence *Journal of Luminescence* **130** 902-909

Spooner N A, Questiaux D G 2000 Kinetics of red, blue and UV thermoluminescence and optically-stimulated luminescence from quartz *Radiation Measurements* **32** 659-666

Wintle A G, Murray A S, 1997 The relationship between quartz thermoluminescence, photo-transferred thermoluminescence, and optically stimulated luminescence *Radiation Measurements* **27** 611-624

## 10. FIGURE CAPTIONS

### Figure 1

Time-resolved OSL off-time and optically stimulated phosphorescence curves from a single aliquot of quartz (WIDG8) measured on different timescales covering over eight decades. (a) The first (black) curve is measured using an on-time of 50  $\mu$ s, an off-time of 500  $\mu$ s (~40,000 pulses) and has a resolution of 50 ns. The second (red) curve is measured using an on-time of 1 ms, an off-time of 5 ms (9,000 pulses) and has a resolution of 6.6  $\mu$ s. The third (blue) curve is measured using an on-time of 0.2 s, an off-time of 7.8 s (a single pulse) and has a resolution of 0.002 s. In all three measurements the aliquot was dosed with 25 Gy followed by a preheat to 260°C for

10 s and blue light stimulation at 125°C. The curves have been normalized to the initial intensity, and the red curve has been reduced by a factor 0.9 and the blue curve by a factor of 0.02 for ease of illustration. Note that the scale is double-log. The curves in (b), (c), and (d) are the semi-log plots of the individual curves from (a). The numbers on the curves 1-4 represent the four major components in the signal which has been identified by visual inspection.

### **Figure 2**

Time-resolved blue light stimulated OSL off-time curves from a single aliquot of quartz (WIDG8) for different preheats in the range: 200°C-300°C in steps of 20°C. The aliquot was dosed with 25 Gy, preheated for 10 s and stimulated at 125°C using an on-time of 1 ms and an off-time of 5 ms. The curves have been normalized to the first point in the off-time. Inset: The off-time decay counts integrated for the periods 0.0-6.6  $\mu$ s (filled circles) and 1005.0-1011.6  $\mu$ s (open circles) and plotted as a function of preheat temperature. For comparison, the two data sets are normalised to their value for the preheat of 200°C.

### **Figure 3**

(a) Time-resolved blue light stimulated OSL off-time curves from a single aliquot of quartz (WIDG8) measured at the temperatures: 50°C-225°C. The aliquot was dosed with 25 Gy and heated to 260°C for 10 s prior to each measurement using an on-time of 1 ms and an off-time of 5 ms. The curves have been normalized to the first point in the off-time. Inset: The same curves shown on a log-log scale. (b) Intensity (triangles) and lifetime (circles) of the component shown as #1 in Fig. 1(a) plotted as a function of stimulation temperature. The intensity is calculated from integrating counts in the initial 0.0-6.6  $\mu$ s of the off-time curve after a background subtraction (the average counts per channel derived from data between 5900 and 5990  $\mu$ s). (c) Intensity (circles) and lifetime (triangles) of the component shown as #2 in Fig. 1(a) plotted as a function of the stimulation temperature. The lifetime in ms was determined from single exponential fitting of the curves after subtraction of an average over the last 50 points and removing the initial 400  $\mu$ s of the off-time. The intensity was calculated at 400  $\mu$ s into the off-time. Note that the open symbols denote recycling point measurements and that the errors on the lifetimes in (b) and (c) are not visible as they are smaller than the size of the symbols.

**Figure 4**

Blue light stimulated OSL off-time curves from a single aliquot of quartz (WIDG8) measured using preheats in the range: 200-300°C in steps of 20°C. The aliquot was dosed with 25 Gy and preheated for 10 s prior to each measurement and stimulated at 125°C using a pulse length of 0.2 s and detecting for 7.8 s following the stimulation pulse. The curves have been normalized to the first point in the off-time. The inset shows the curves on a log-log scale.

**Figure 5**

(a) Blue light stimulated OSL off-time curves from a single aliquot of quartz (WIDG8) measured in the temperature range: 50-200°C. The aliquot was dosed with 25 Gy and heated to 260°C for 10 s prior to each measurement using a stimulation pulse length of 0.2 and detecting for 7.8 s following the stimulation pulse. The curves have been normalized to the first point in the off-time. (b) The initial 3 s of the curves from (a) labelled with letters from a - f to indicate the behaviour of the OSP from the 110°C TL peak (see text for details).

**Figure 6**

(a) Summary of lifetimes (found from fitting the initial 3 s of the curves in Fig. 5 with a sum of three exponentials) on an Arrhenius plot. The natural logarithm of the lifetimes for fast (circle) medium (triangle) and slow (square) components derived from fitting are plotted against the inverse of stimulation temperature (times Boltzmann's constant). (b) Summary of lifetimes found from fitting the remaining part of the off-time decays in Fig. 5 after subtraction of a constant term. The curves could be adequately fitted with a single decaying exponential. Note that the errors on the lifetimes in both (a) and (b) are not visible as they are smaller than the size of the symbols.

**Figure 7**

TL curves showing the effect of photo-transfer in quartz (WIDG8) due to short blue light stimulations of different length. An aliquot of quartz was dosed with 25 Gy, heated to 300°C for 10 s, blue light stimulated at 20°C, and then a TL curve to 300°C was measured using a heating rate of 2°Cs<sup>-1</sup>. The same cycle was repeated with 0 s of

light stimulation before the TL measurement. The curves shown in the figure have all been obtained by subtraction of TL before illumination from that after illumination. Repeat measurements showed less than 2% variability.

### Figure 8

Off-time curve decay rate change ('kink') as a function of stimulation pulse duration. An aliquot of quartz (WIDG8) was dosed with 25 Gy, preheated to 260°C for 10 s and stimulated at 100°C with a single on-pulse of varying length between 0.1 s and 1.6 s. The curves have been normalized to the initial off-time point. Inset: Position of the 'kink' in the off-time curve as a function of stimulation pulse duration.

### Figure 9

Band diagrams showing (a) A three trap ( $T_1$ ,  $T_2$ , and  $T_3$ ) - one recombination centre (L) model. The traps  $T_1$ ,  $T_2$ , and  $T_3$  have initial concentrations and decay constants  $n_1$ ,  $\lambda_1$ ,  $n_2$ ,  $\lambda_2$ , and  $n_3$ ,  $\lambda_3$  respectively, and  $f$  represents the fraction of charge transfer from one energy level to the other (b) A one trap ( $T_3$ ) - two recombination centres ( $L_a$  and  $L_b$ ) model.  $L_a$  has two excited states,  $L_{a2}$  and  $L_{a1}$ . The same subscript notation is used as in (a) for concentrations and decay constants for the trap and the excited states.

### Figure 10

(a) Curves showing the loss from  $T_3$ ,  $T_2$ , and  $T_1$  together with the phosphorescence emitted at L when solving the rate-equations (1)-(4) using the parameters:  $n_{10} = 50 \text{ cm}^{-3}$ ,  $\lambda_1 = 0.04 \text{ s}^{-1}$ ,  $n_{20} = 300 \text{ cm}^{-3}$ ,  $\lambda_2 = 0.09 \text{ s}^{-1}$ ,  $n_{30} = 25 \text{ cm}^{-3}$ ,  $\lambda_3 = 0.3 \text{ s}^{-1}$ , and  $f_3 = 0.1$ , and  $f_2 = 0.92$ . (b) The same curves from (a) shown on a semi-log scale.

### Figure 11

Curves showing the phosphorescence emitted at L when running the rate-equations (5)-(7) using the parameters:  $n_{10} = 50 \text{ cm}^{-3}$ ,  $\lambda_1 = 0.04 \text{ s}^{-1}$ ,  $n_{20} = 300 \text{ cm}^{-3}$ ,  $\lambda_2 = 0.09 \text{ s}^{-1}$  for different values of  $f$  between 0.1 and 1. The loss from  $T_2$  and  $T_1$  together with the light emitted from L for  $f = 0.3$  are shown inset to illustrate the dependence between the three.

### Figure 12

Normalized cumulative phosphorescence (integrated over 10 s) following different lengths of CW stimulations in the range of 10 s to 70 s. The sample was dosed with 25 Gy, preheated to 260°C for 10 s and stimulated at 125°C. The dashed line indicates the dark count level also integrated over 10 s. Inset: The percentage ratio between the end point of the OSL curve and the first point in the phosphorescence signal given for different CW stimulation times.

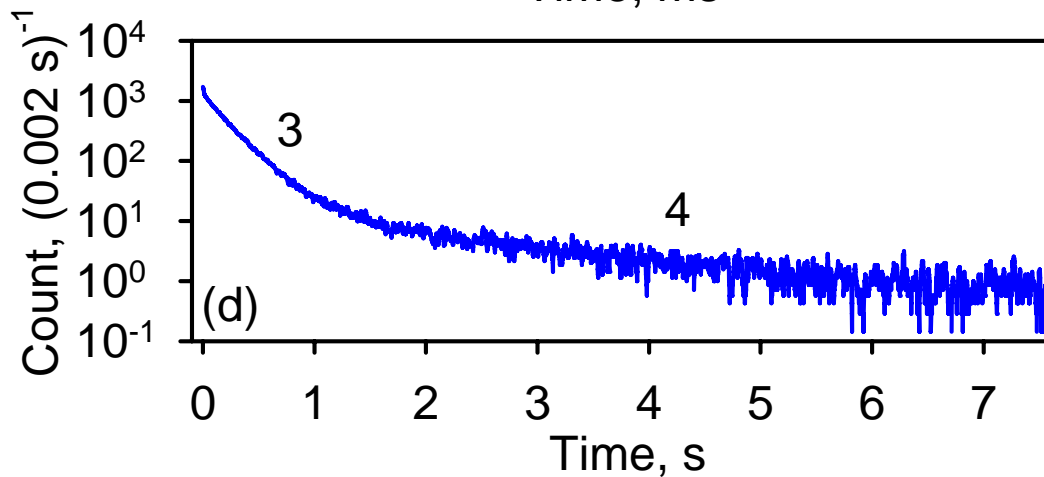
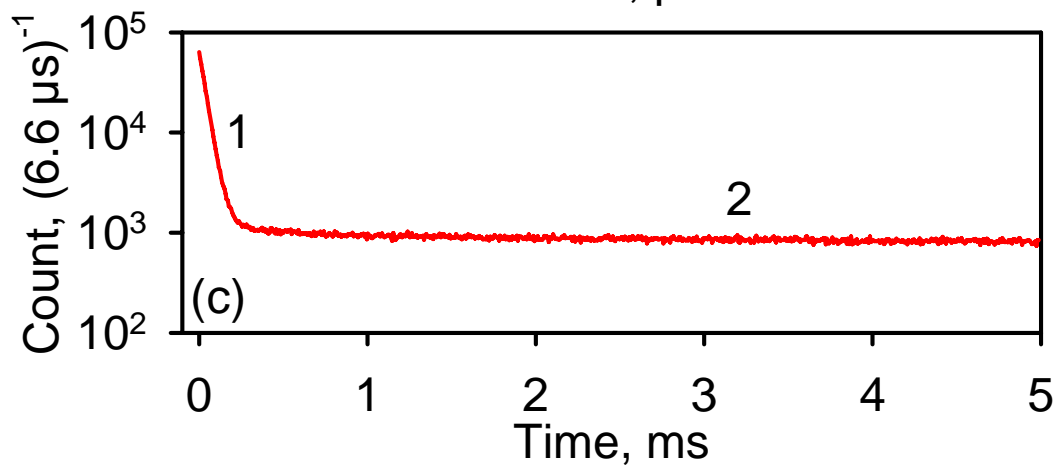
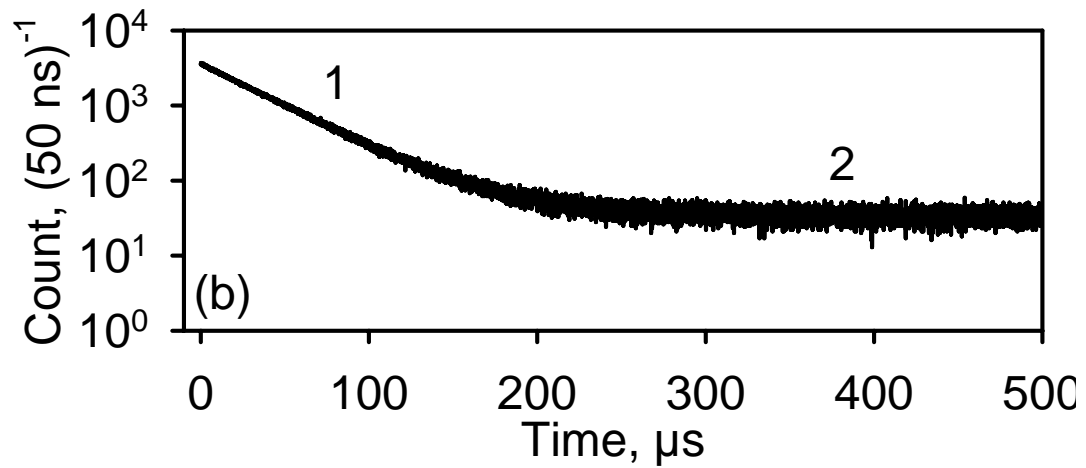
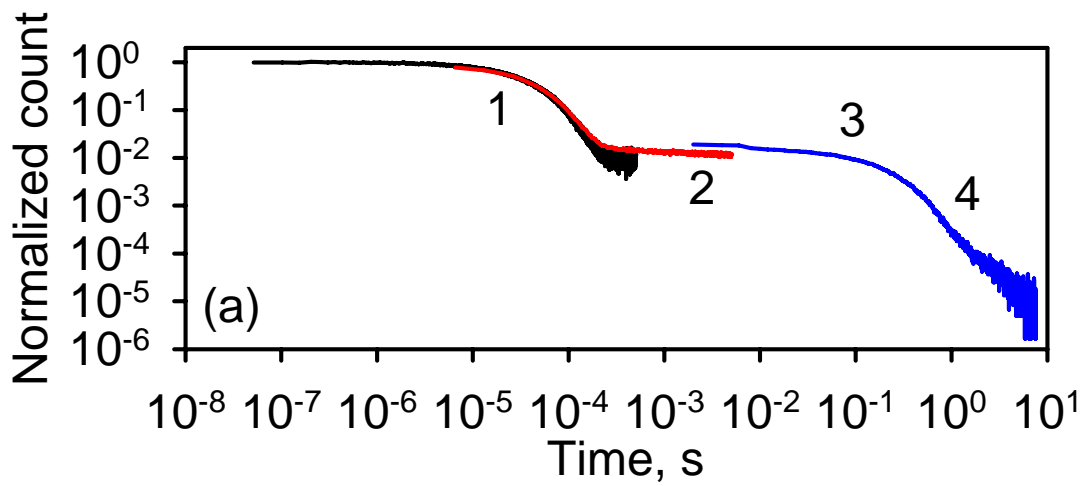


Figure 1 (Figure1.eps)

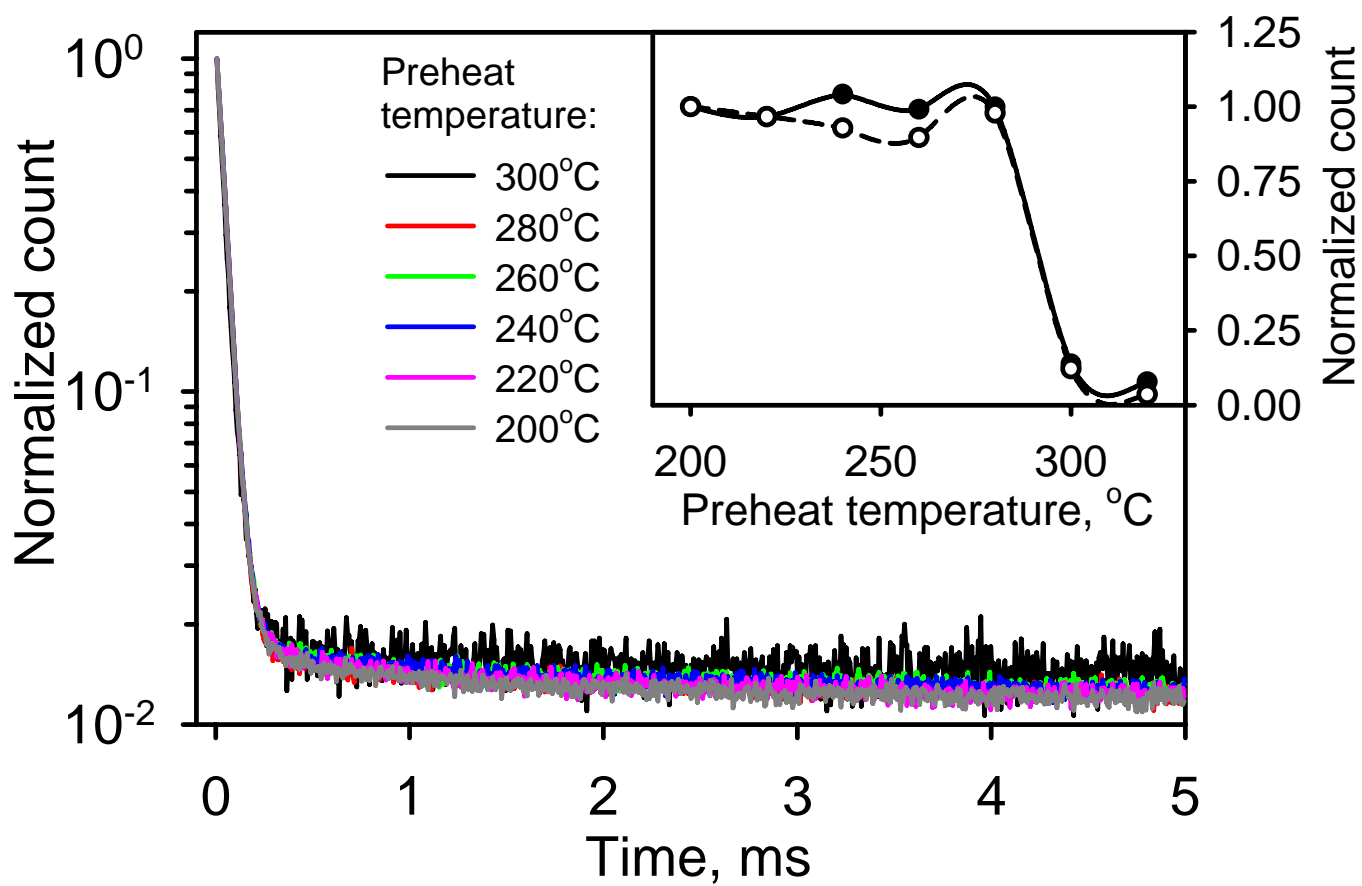


Figure 2 (Figure2.eps)

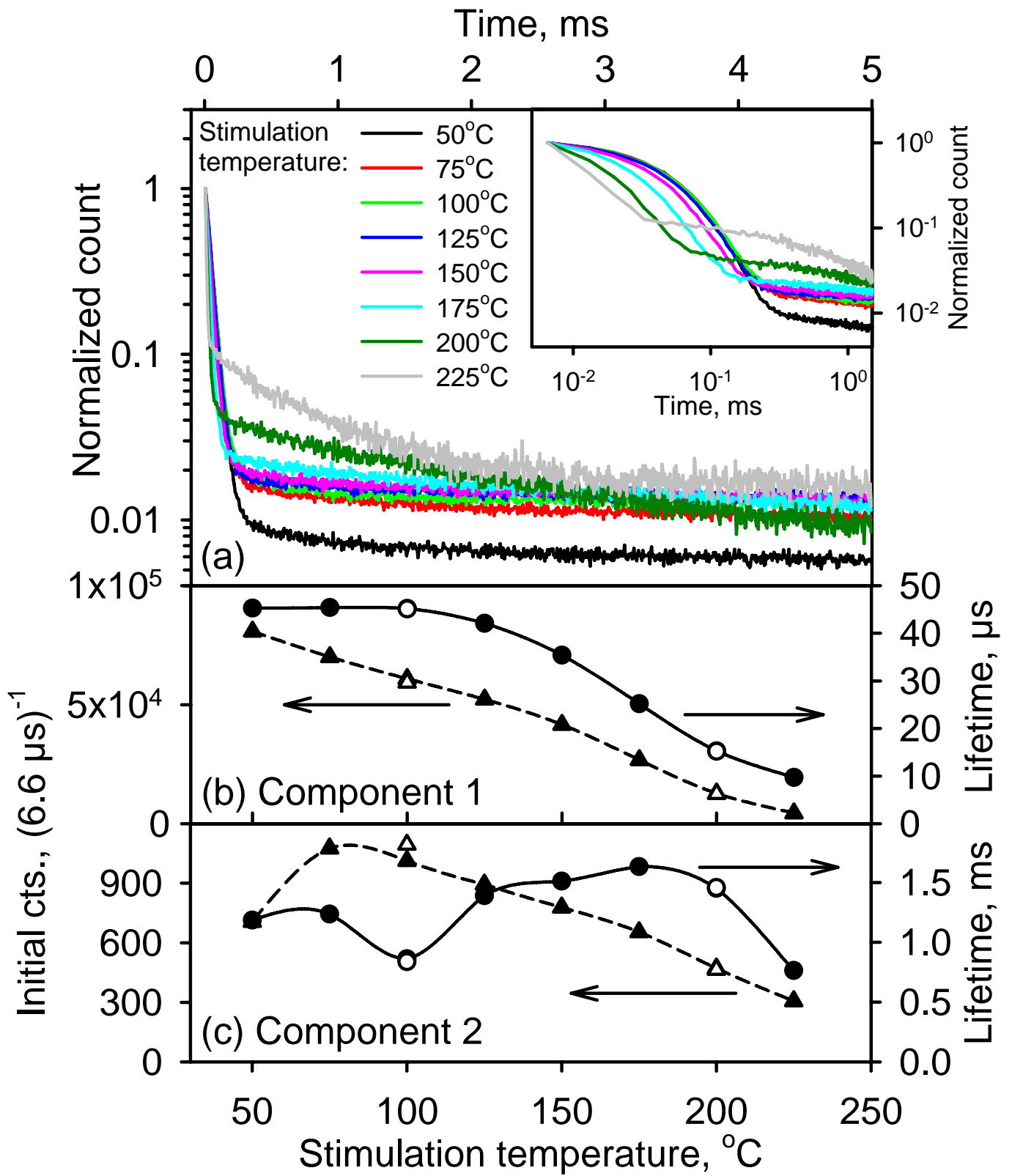


Figure 3 (Figure3.eps)

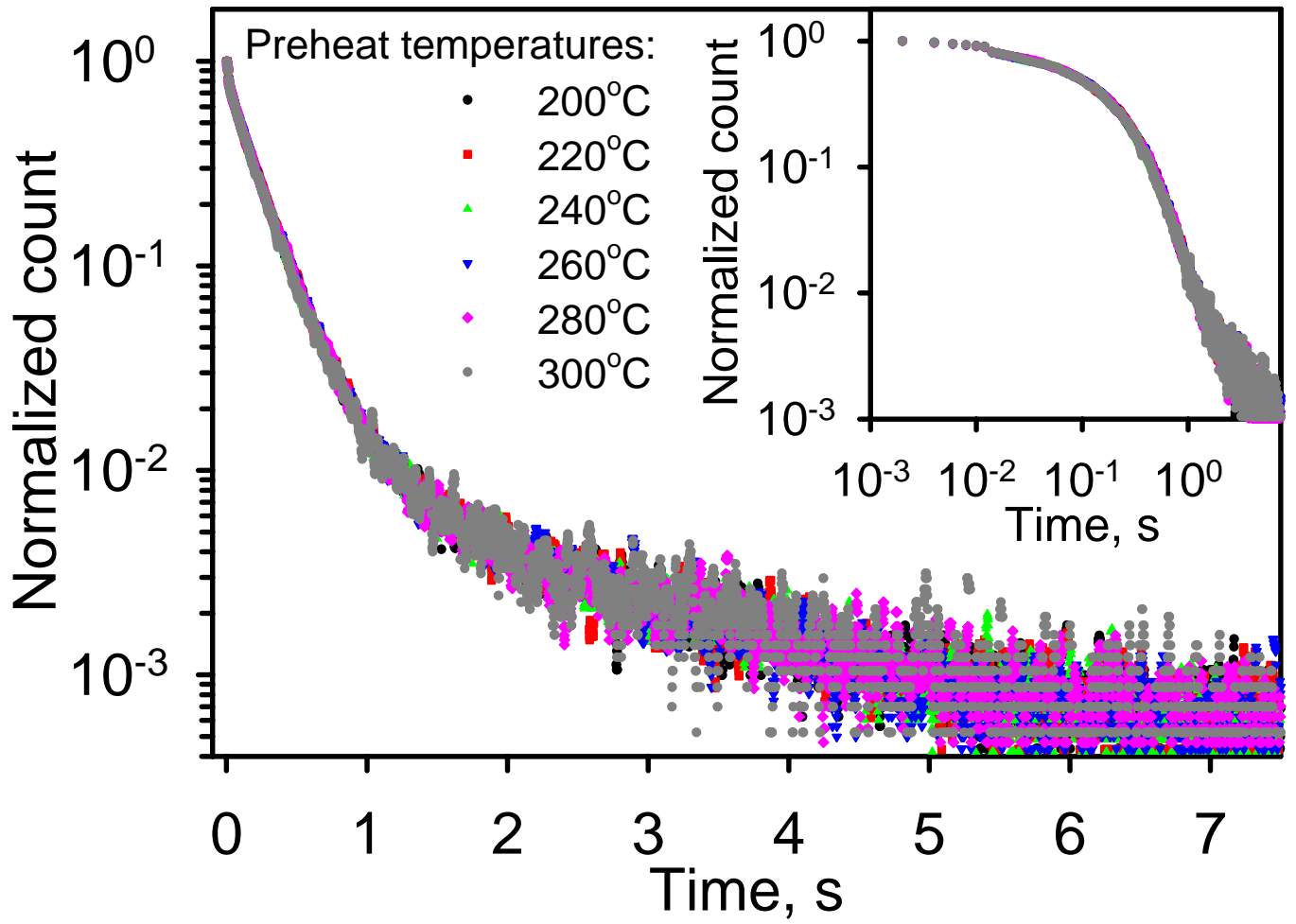


Figure 4 (Figure4.eps)

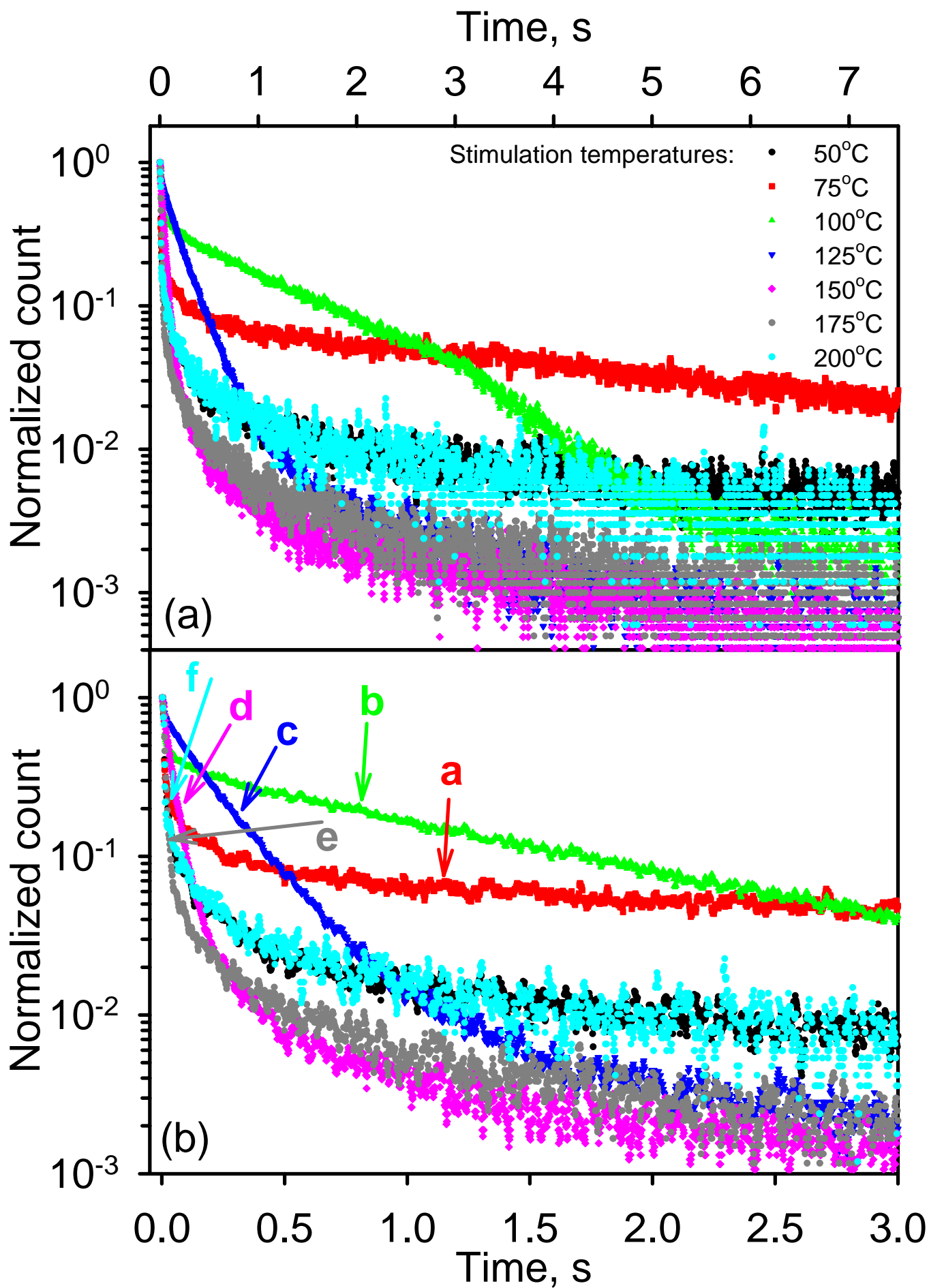


Figure 5 (Figure5.eps)

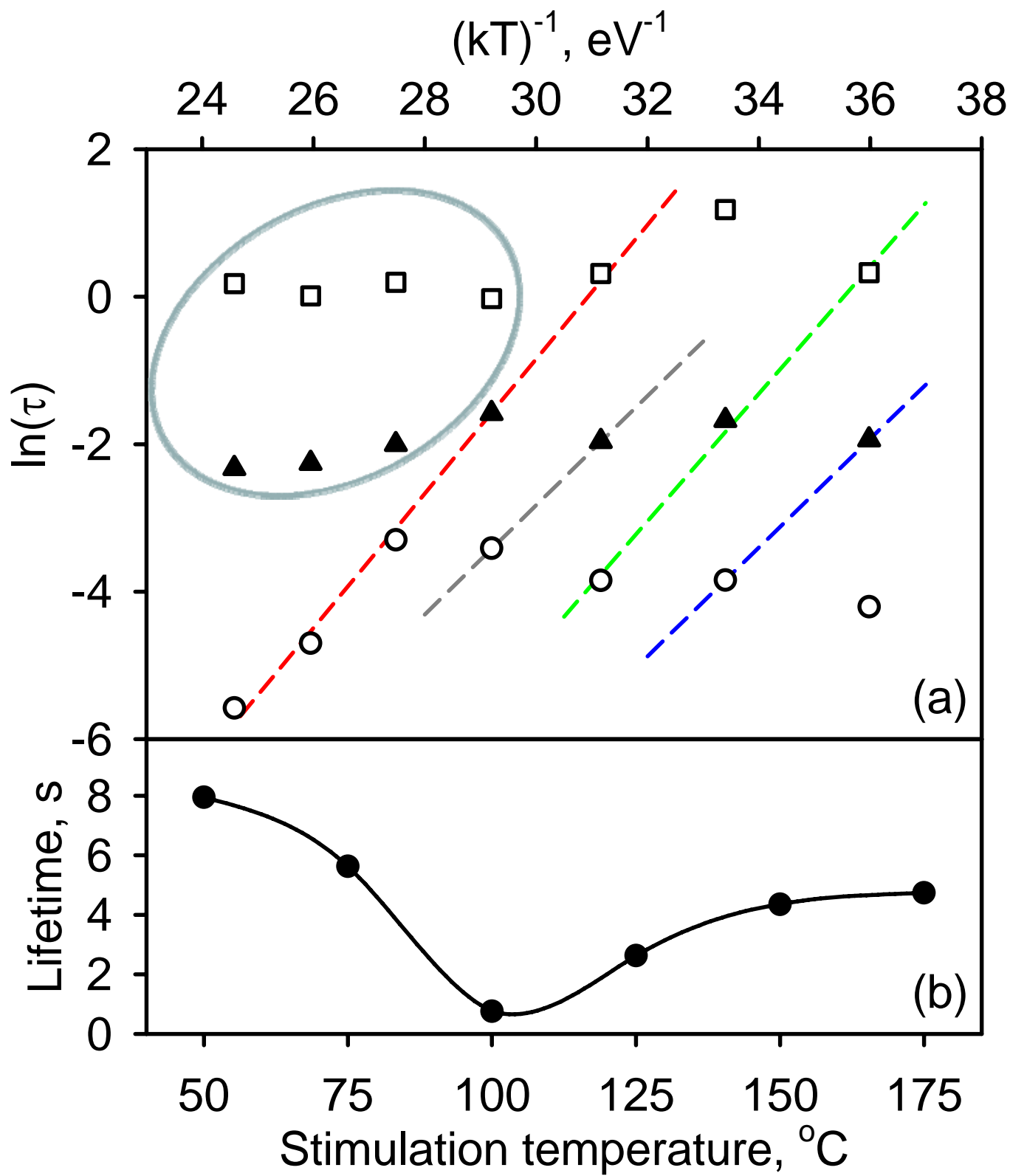


Figure 6 (Figure6.eps)

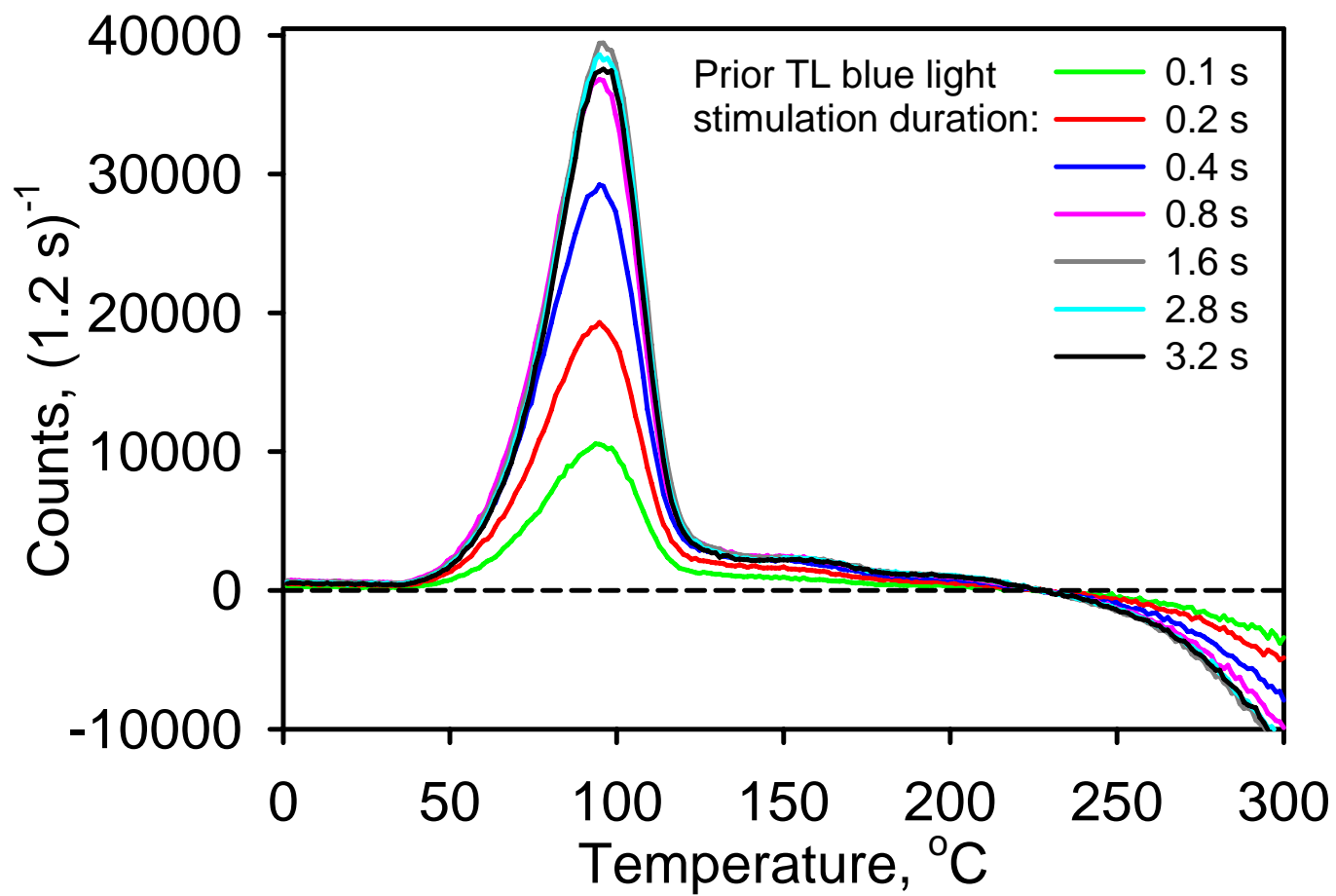


Figure 7 (Figure7.eps)

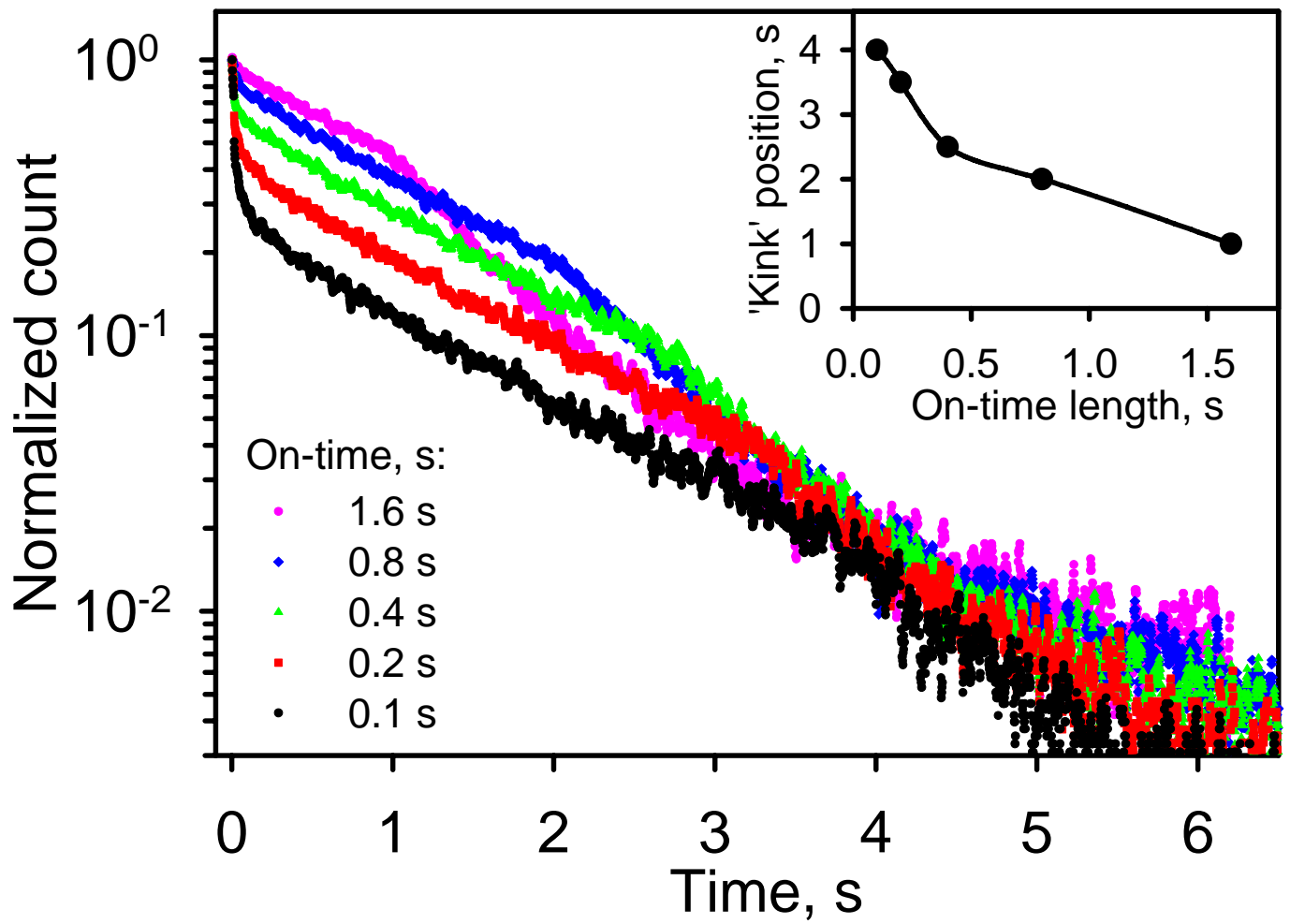


Figure 8 (Figure8.eps)

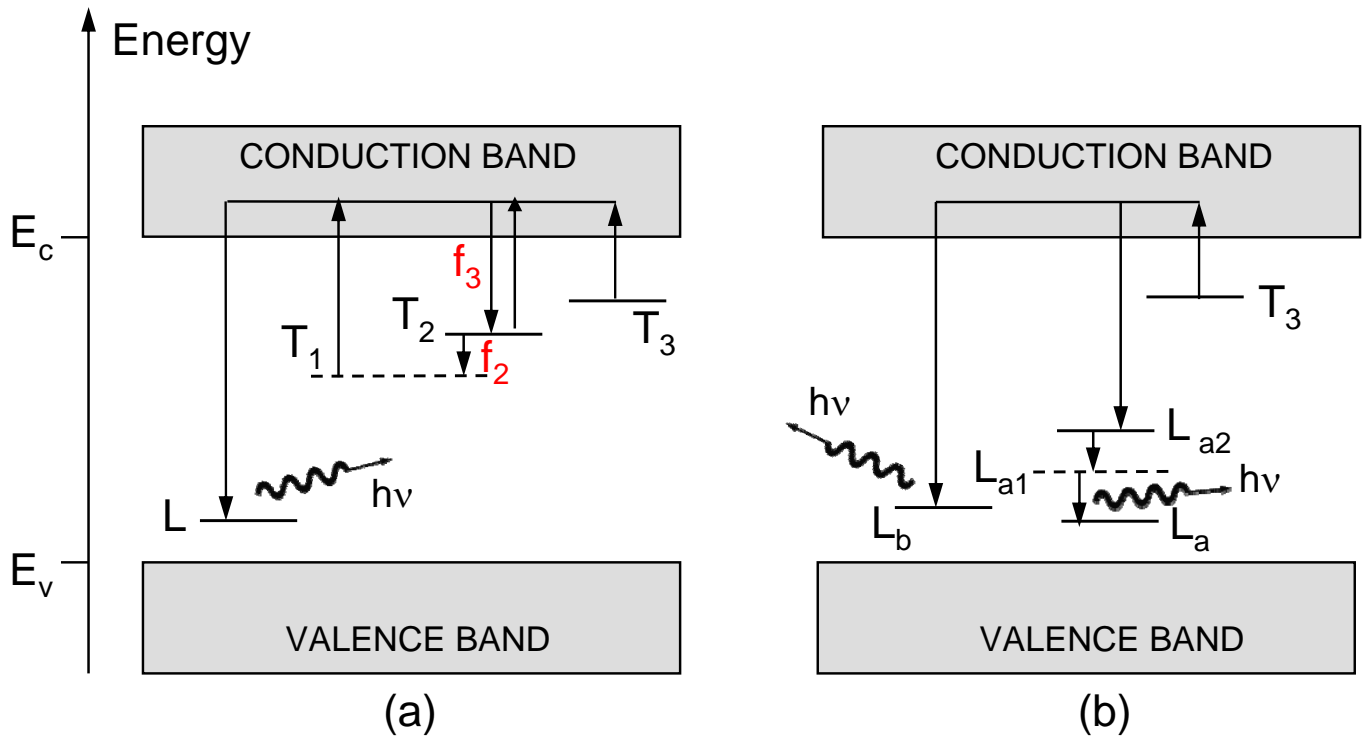


Figure 9 (Figure9.eps)

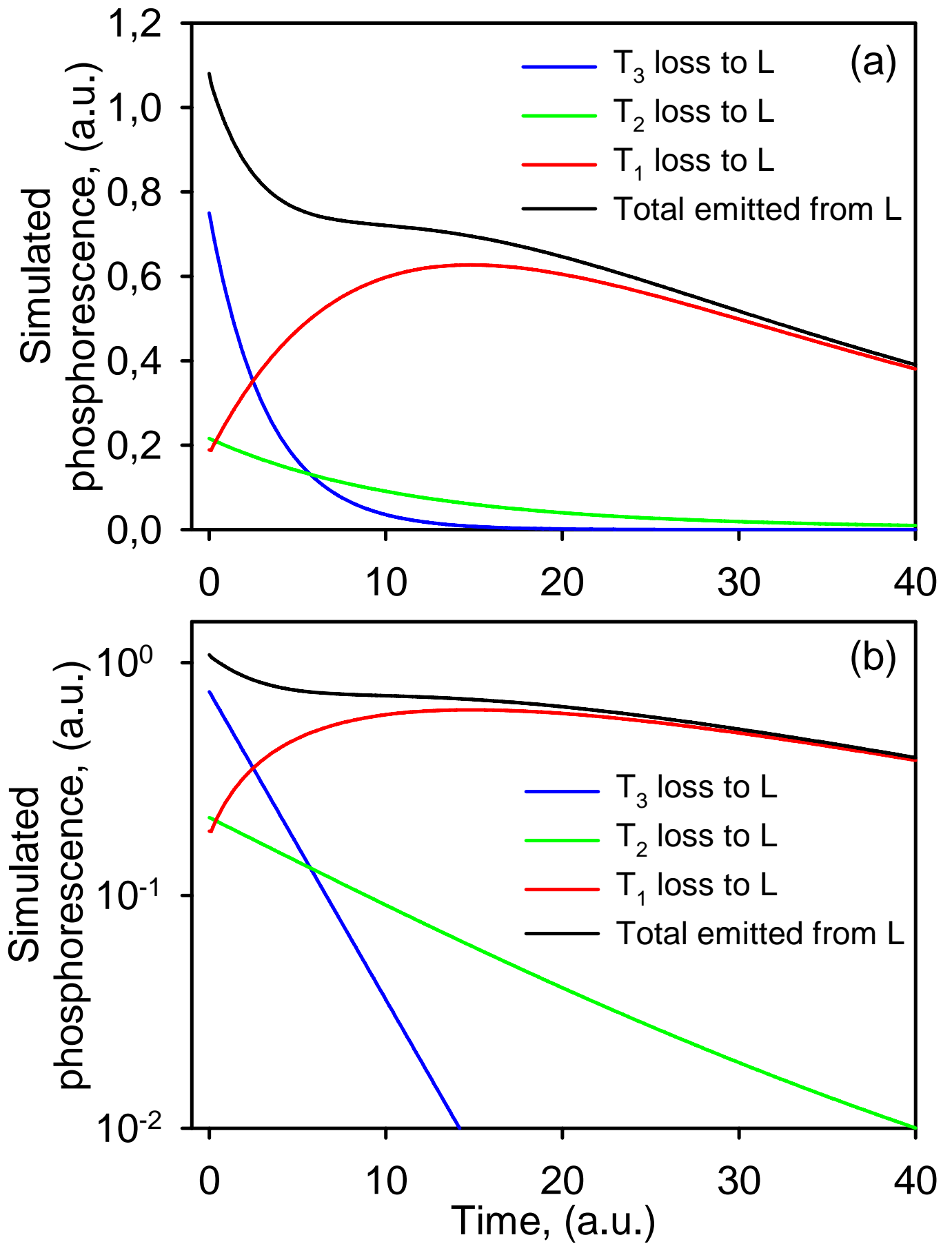


Figure 10 (Figure10.eps)

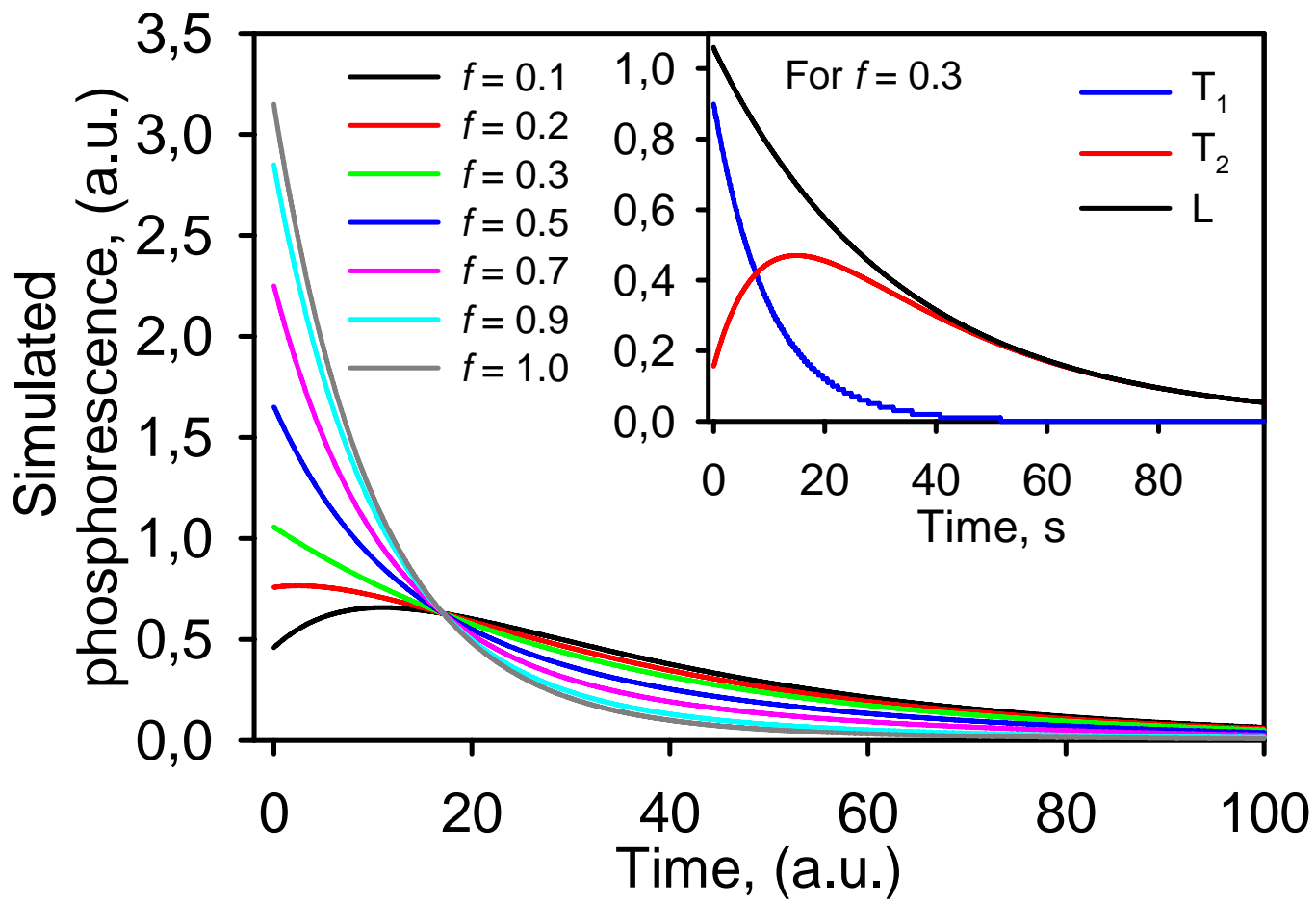


Figure 11 (Figure11.eps)

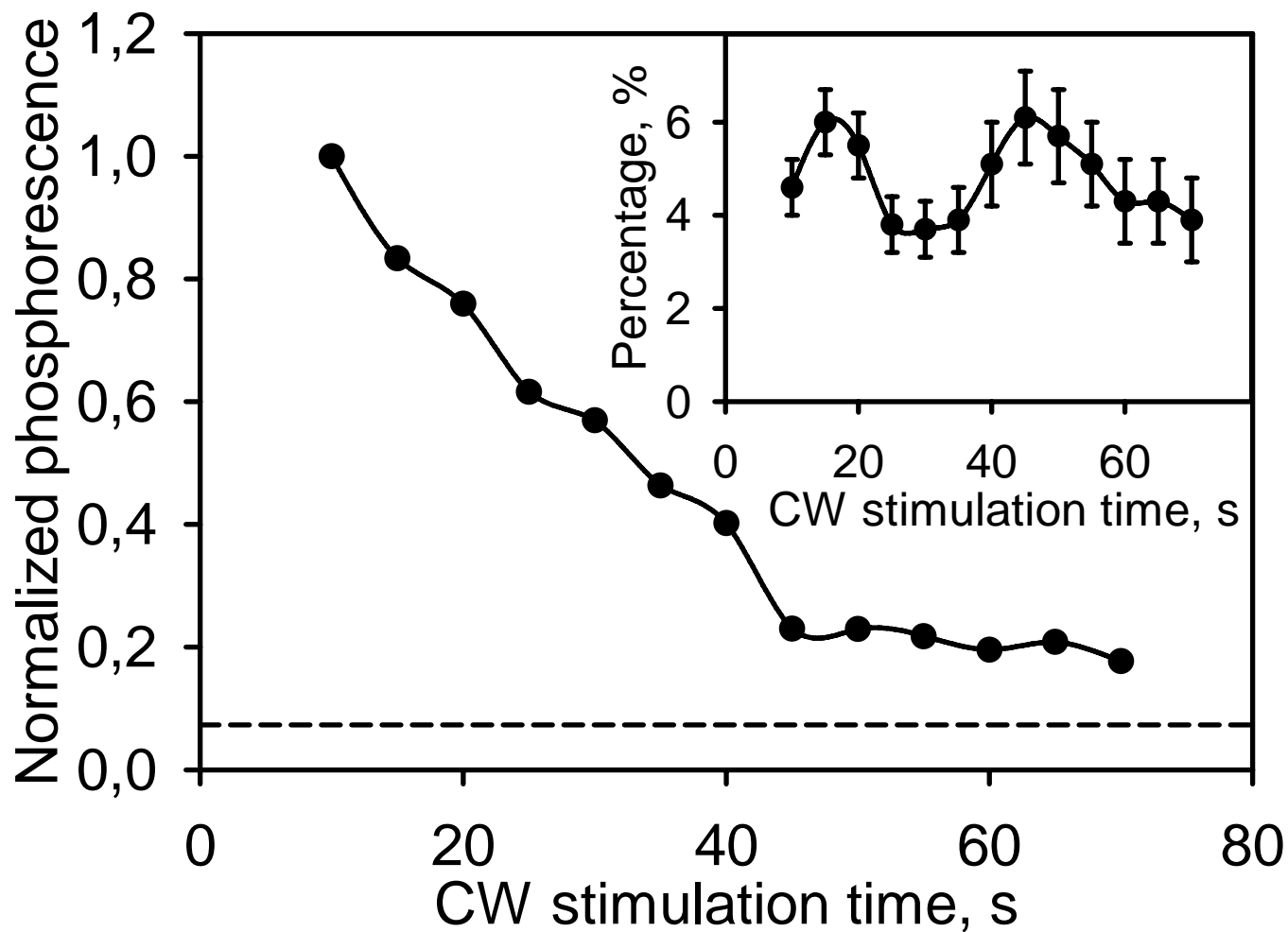


Figure 12 (Figure12.eps)